Journal of Structural Geology 32 (2010) 1943–1959

Contents lists available at ScienceDirect

Journal of Structural Geology

journal homepage: www.elsevier.com/locate/jsg

Quantifying diagenetic and stratigraphic controls on fracture intensity in platform carbonates: An example from the Sierra Madre Oriental, northeast Mexico

Orlando J. Ortega [a,*], Julia F.W. Gale [b], Randall Marrett [c]

[a] Shell International E&P, 150 North Dairy Ashford, A-1014 Houston, TX 77079, USA
[b] Bureau of Economic Geology, Jackson School of Geosciences, The University of Texas at Austin, TX 78713, USA
[c] Department of Geological Sciences, Jackson School of Geosciences, University of Texas at Austin, 1 University Station C1100, Austin, TX 78712, USA

ARTICLE INFO

Article history:
Received 30 September 2009
Received in revised form
29 June 2010
Accepted 2 July 2010
Available online 14 July 2010

ABSTRACT

Normalized fracture intensity measured along 1D scanlines was used to compare fracture intensity for different sedimentary facies, stratigraphic position, bed thickness and degree of dolomitization in carbonate beds of the Cupido and Tamaulipas formations, northeast Mexico. We calculated the fracture intensity for individual beds, for single and combined fracture sets, and the statistical significance of relationships using bivariate weighted regressions and multivariate methods. Results suggest that the degree of dolomitization is positively correlated with fracture intensity and has the strongest correlation, followed by the position of the bed in the stratigraphic cycle and the mud content. Dolomite content, normalized position in the parasequence, environment of deposition, and mud content show a significant degree of correlation among themselves and should be considered dependent variables for statistical purposes. Geological observations suggest that dolomite precipitation and fracturing occurred, at least in part, synchronously in these rocks. A fracture-intensity distribution model integrating sequence-stratigraphic and diagenetic history is proposed for the Cupido and Tamaulipas formations with potential use in similar carbonate successions. Our analysis does not support the classic bed-thickness–fracture-spacing relationship.

1. Introduction

Fracture intensity (abundance) is one of the key parameters needed for an understanding of fluid flow in otherwise low-permeability rocks, yet it is difficult to measure directly in the subsurface because of sampling problems. Predictive models (e.g., Mueller, 1991; Rives et al., 1992; Fischer et al., 1995; Bai and Pollard, 2000; Philip et al., 2005) require testing with datasets that face the same problems. Nelson (2001) identified the principal geologic controls on fracture intensity as (1) composition, (2) texture (including grain size and porosity), (3) stratigraphy (bed thickness), and (4) structural position. Structural position has been the subject of many studies of fracture intensity (e.g., Antonellini and Mollema, 2000; Casey and Butler, 2004; papers in Hennings, 2009). Although structural effects are locally important in the folded platform-carbonate rocks of the Sierra Madre Oriental, Mexico, our focus is on diagenetic, bed thickness and stratigraphic controls on fracture intensity. We selected outcrops in the same structural position in the limb region of kilometer-scale folds, away from hinges, and where bedding dip is constant. Variation of fracture intensity between outcrops due to structural position is therefore minimized. We used a size-normalized fracture-intensity measurement method described by Ortega et al. (2006). Normalized fracture intensity is determined in the context of varying sedimentary facies, dolomite content, bed thickness, and position of beds in fifth-order stratigraphic cycles. We attempted to answer the following questions. Which stratigraphic parameters exert the strongest control on fracture intensity? Is there a predictable pattern of fracture-intensity distribution?

2. Previous fracture-intensity studies

Compositional controls on fracture intensity have been studied in laboratory experiments (e.g., Handin et al., 1963) and in outcrops and core (Das Gupta, 1978; Sinclair, 1980; Narr, 1991; Gillespie et al., 1993, 1999, 2001; Mandal et al., 1994; Nelson and Serra, 1995; Nelson, 2001). Handin et al. (1963) found that fracture intensity decreases from quartzites to dolostones, to sandstones, to limestones, and that the increase in ductility with burial is greater for limestones than for other sedimentary rocks. Sinclair (1980) suggested that fine-grained carbonates have higher fracture intensity

* Corresponding author.
E-mail address: Orlando.Ortega@Shell.com (O.J. Ortega).

0191-8141/$ – see front matter © 2010 Elsevier Ltd. All rights reserved.
doi:10.1016/j.jsg.2010.07.004

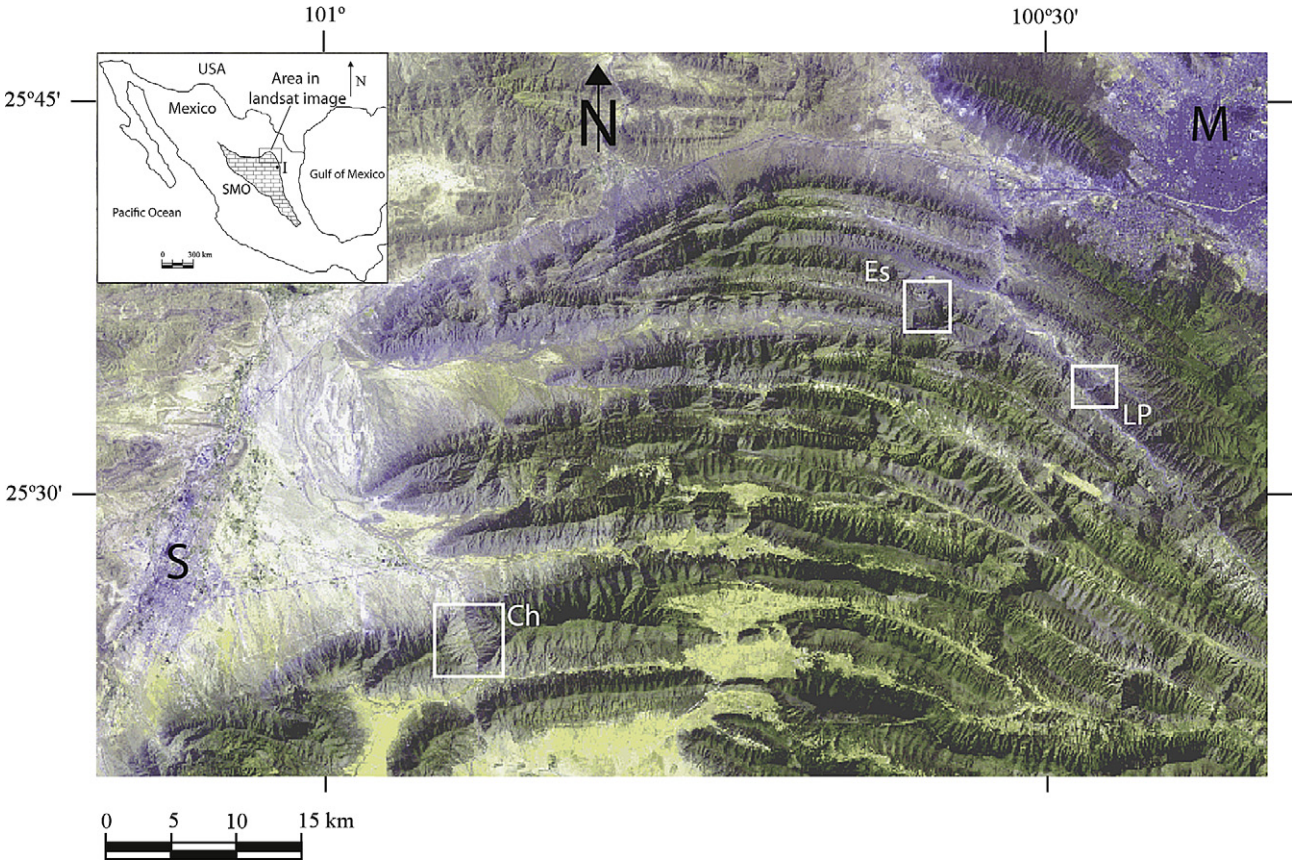

Fig. 1. Landsat image of the Monterrey salient in the Sierra Madre Oriental (SMO) showing kilometer-scale folds affecting Mesozoic rocks. Ridges are dominated by carbonates of the Cupido and Tamaulipas Superior formations. Study locations are in canyons that cut across anticlines. Ch: El Chorro, Es: La Escalera, LP: Las Palmas, M: Monterrey, S: Saltillo. Inset: map of Mexico showing location of landsat image. I: Iturbide.

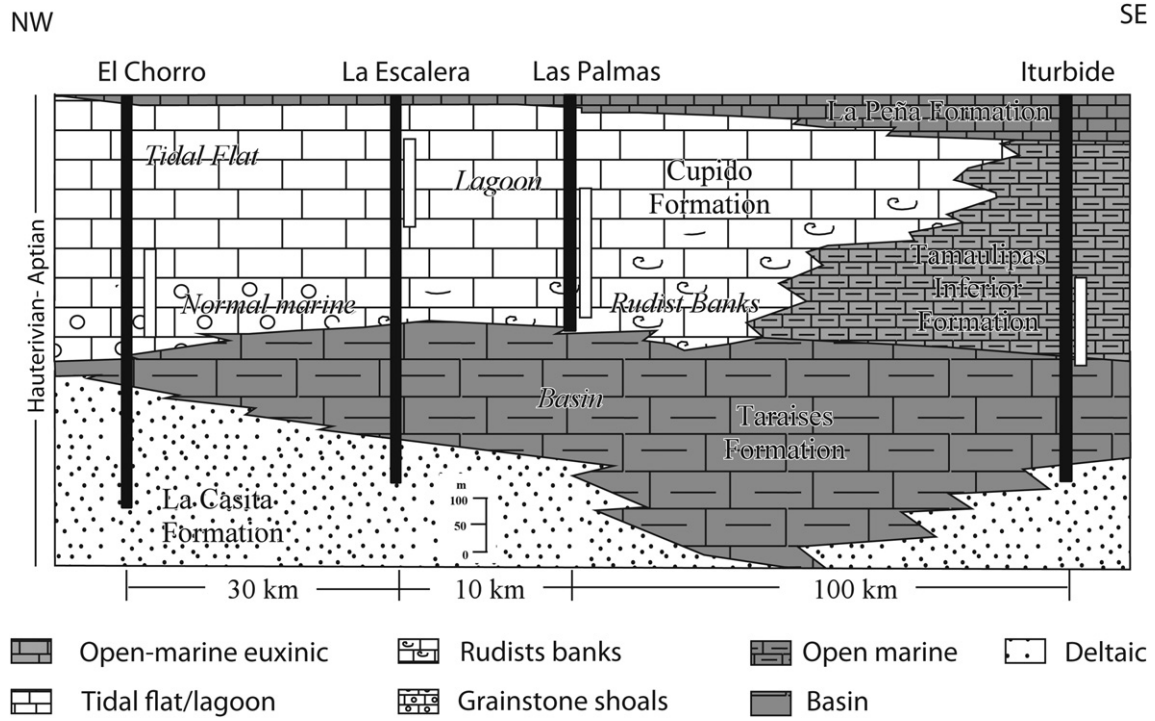

Fig. 2. NW-SE schematic stratigraphic section across the Cupido–Tamaulipas platform (modified from Wilson et al., 1984). Black columns show the approximate stratigraphic interval exposed in each area. White columns indicate the approximate section studied at each location. Horizontal distances between localities not at uniform scale.

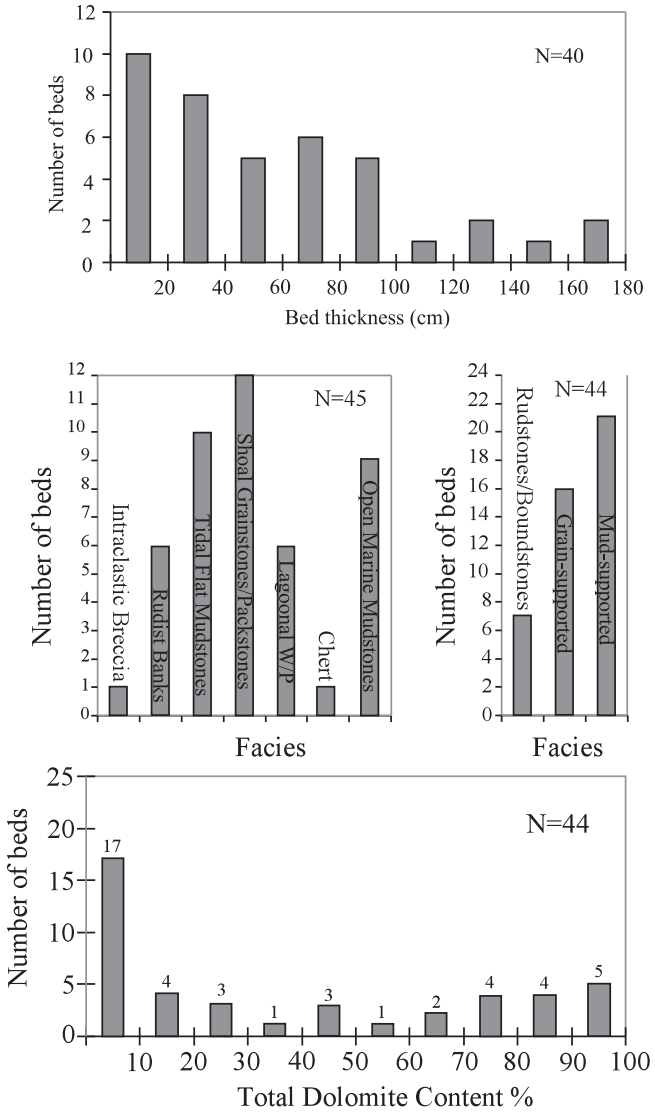

Fig. 3. Variation of facies, bed thickness, and dolomite content among layers studied. The facies definition includes textural groups and depositional environment interpretations. Some histograms exclude multifacies beds and/or chert beds. Total dolomite content is based on thin-section point counting. From Ortega et al. (2006).

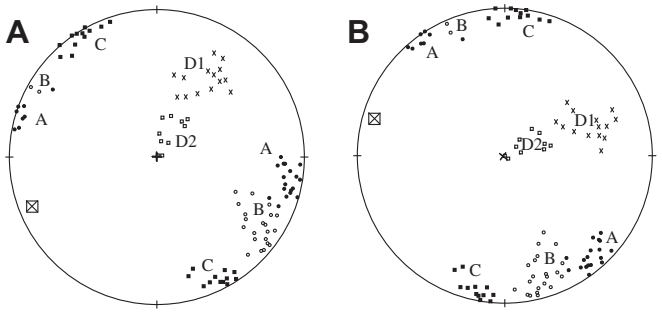

Fig. 5. Unfolded fracture orientation data, El Chorro Anticline. (A) Unfolding about a horizontal fold axis. (B) Further rotation of 38° clockwise about a vertical axis as suggested by palaeomagnetic data (Kleist et al., 1984). Fracture sets D1 and D2 are youngest and are probably associated with folding. Fracture sets A, B, and C probably formed when bedding was horizontal. Set C lies subparallel to the fold axis and may have been formed during the shortening event that produced the fold.

than coarse-grained carbonates. Das Gupta (1978) concluded that greater dolomitization correlates with higher fracture intensity; although dolomitized beds were thinner than limestone beds in that study and separation of bed thickness from dolomitization effects on fracture intensity is difficult.

Carbonate mechanical and fracture stratigraphy was addressed by Corbett et al. (1987), Ferrill and Morris (2008), Laubach et al. (2009), and several papers in a special issue of the *Journal of Structural Geology*, "Deformation in Carbonates" (Agosta and Tondi, 2009). For example, Zahm et al. (2010) used integration of facies, rock strength, and mud content within a sequence-stratigraphic framework as a means of predicting faulting and jointing in limestone outcrops. Their study found that "fracture deformation intensity" was higher in transgressive system tracts (TST) than in highstand system tracts (HST). The TST in that study also had more argillaceous, thinner cycles and rocks with lower unconfined strength. There was, however, no dolomitization component in their example and as we will show here, dolomitization overrides facies and mud-content controls on fracture intensity.

3. Study area

The study area is in the north-central part of the Sierra Madre Oriental (SMO) fold and thrust belt in northeastern Mexico (Fig. 1). An Upper Hauterivian–Lower Aptian platform-to-basin carbonate system, comprising the Cupido, Tamaulipas Superior, and

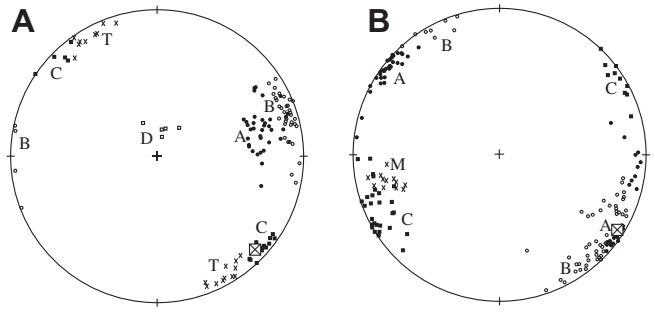

Fig. 4. Unfolded fracture orientation data, San Blas Anticline. (A) La Escalera; (B) Las Palmas. Simple rotations of poles to fractures around fold axis restoring bedding to horizontal. Fold axis is indicated by a crossed large square. Restoration reveals two dominant fracture orientations approximately 60–70° apart. Crosscutting relationships between sets A and B are mutual suggesting that these sets are synchronous. Set C crosscuts sets A and B at both localities. Set D restores to a horizontal attitude suggesting it might be related to tectonic stylolites and folding. T are poles to tectonic stylolites and M are poles to late, mud-filled fractures.

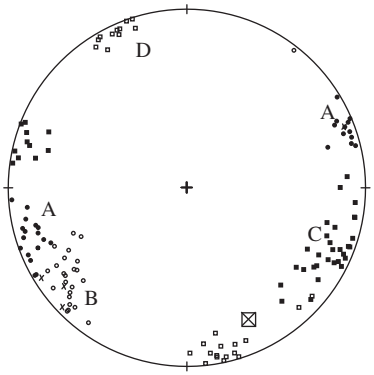

Fig. 6. Unfolded fracture orientation data, Iturbide Anticline. Unfolding is about a fold axis plunging 20° southeast. Fracture set D is the youngest and is probably associated with tectonic stylolites (T) and folding. Fracture sets A, B, and C probably formed when bedding was horizontal – they are close in orientation to similarly labeled sets at other locations.

Table 1
Summary of number of fractures measured and scanline lengths.

Locality	Bed number	Apertures measured				Scanline length (mm)			
		Set A	Set B	Set C	Set D	Set A	Set B	Set C	Set D
Escalera	1	202	148			705	1511		
	2	233	219			1024	1568		
	3	229	241			1689	959		
	4		206				1537		
	5B			62				8331	
	6A	8		9		2007		2667	
	6B	200	240			1422	2311		
	7	210	205			1918	1372		
	8	218	213			927	851		
	9	204	224			1664	1588		
	10		84				13183		
	11		202				12370		
	12	206	197			876	921		
Iturbide	1	215			61	3721			6223
	2	189		86		2400		5169	
	3			166	204			4267	7734
	4			163	194			6566	5283
	5	182				2261			
	6			210				2921	
	7			389				3810	
	8				411				2394
	9			220	200			4559	5207
	10	233		220	210	3683		7988	5639
Palmas	1	21	217			2276	2578		
	2	223	30			5639	5146		
	3		59	248			3602	3975	
	4	121		19		6807		1532	
	5	93		72		5194		2438	
	6	219		33		2032		1077	
	7	109		112		5458		9068	
	8	204		24		1702		2921	
	9	206		115		1727		2096	
	10	222		206		1715		3073	
Chorro	1		213		23		4547		5004
	2			225	210		1219		2515
	3	219	207			3239	3315		
	4	65	215			1278	1524		
	5	212	57	70		2718	2616	2616	
	6	203	51	49		5499	6248	5258	
	7	213		48		1511		3302	
	8	200		43		5067		4389	

Tamaulipas Inferior Formations, is deformed by Laramide-age kilometer-scale folds (Fig. 2). Two of the folds studied are located within the Monterrey Salient (El Chorro and San Blas Anticlines), and one fold (Iturbide Anticline) is located in the north-northwest-oriented ranges of the SMO, ~115 km southeast of Monterrey (Fig. 1). The deformation style is primarily thin-skinned deformation, with a lower detachment probably located in Upper Jurassic gypsum-anhydrite evaporite layers (Marrett and Aranda-García, 1999), except for the Iturbide Anticline, where the evaporite is absent.

3.1. Fracture origin and timing in the Sierra Madre Oriental

Fracture intensity in the San Blas Anticline shows moderate to weak correlation with fold-related layer curvature, and high-fracture-intensity zones do not always correlate with fold hinges (Camerlo, 1998). In El Chorro there is no obvious control of fold geometry on fracture intensity. Although variations in mechanical properties within a layer or fracture clustering within a fold limb cannot be ruled out (Fischer and Jackson, 1999; Olson et al., 2009), study of the San Blas and El Chorro Anticlines suggests that most fold-related strain was accommodated by layer-parallel faults, and enhanced fracturing due to folding occurs only within a few meters of regional-scale hinges (Camerlo, 1998).

The lack of correspondence between fold geometry and fracture intensity is consistent with the inference suggested by Marrett and Laubach (2001) that many fractures in the Cupido Formation predate Laramide folding. Evidence includes fractures from the sets we studied that are present in rotated blocks in collapse breccias in the Cupido Formation; these fractures therefore formed before brecciation. Goldhammer et al. (1991) associated these collapse breccias with fluctuations of sea level during sedimentation.

3.2. Stratigraphy and cyclic sedimentation

The sections studied (Fig. 2) represent laterally correlative Cupido and Tamaulipas Inferior Formations comprising several facies (Conklin and Moore, 1977; Wilson et al., 1984). Shallow-water carbonate sediments prograded over open-marine carbonates of the Taraises Formation, which was deposited in deeper water conditions and overlies clastics of the La Casita and Carbonera Formations near the Coahuila High (Lehmann et al., 1998, and references therein). The El Chorro and La Escalera sections are

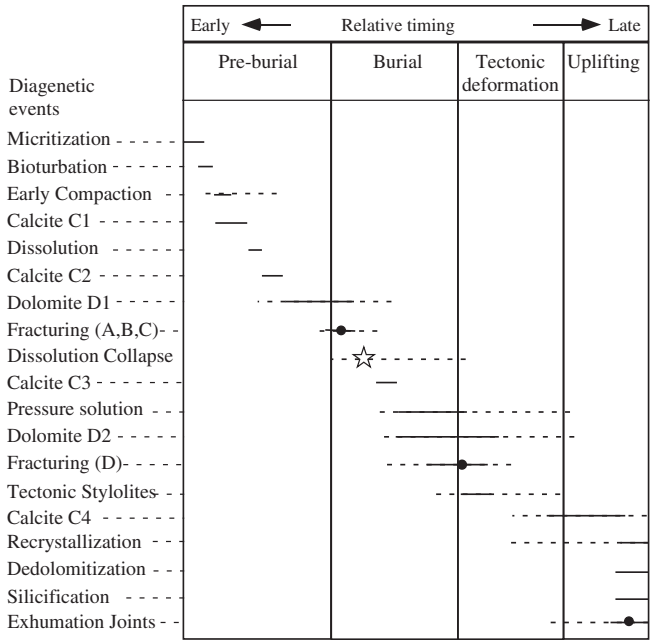

Fig. 7. Paragenetic sequence for shallow-water facies of the Cupido Formation at El Chorro, La Escalera and Las Palmas. Fracturing events in the diagenetic history of the Cupido Formation (modified from Monroy et al., 2001). *Star*: most probable timing for breccia collapse. *Black dots*: interpreted timing for fracturing events. *Dashed line*: possible extent of event. *Solid line*: probable timing on the basis of field observations, petrography and kinematic analyses (Ortega, 2002).

dominated by lagoonal and intertidal carbonate facies. The Las Palmas section contains abundant bivalve bioherms and grainstone shoals of the platform's outer margin. The section at Iturbide is composed mainly of open-marine, deeper water, fine-grained carbonates of the Tamaulipas Inferior and Taraises Formations (Wilson et al., 1984; Goldhammer et al., 1991, and references therein).

Sedimentation in the inner platform facies of the Cupido Formation is cyclic (Wilson et al., 1984; Goldhammer, 1999, Lehmann et al., 1998) and has been interpreted as an effect of climatic and autogenic processes on Milankovitch-driven eustatic sea-level fluctuations (Lehmann et al., 1998). Each parasequence comprises an upward-shallowing succession of lagoonal burrowed limestones on top of hard grounds or sedimentary breccias, followed by grainstone shoals or rudist bioherms, and is capped by cryptalgal/microbial laminites and/or evaporites. By quantifying textural, diagenetic, and rock-composition controls on opening-mode fracture intensity, we also assess to what degree the underlying architecture of a carbonate platform may be used to predict fracture stratigraphy and intensity.

3.3. Diagenesis

Most dolomitized layers are at or near the tops of parasequences, suggesting focused, localized dolomitization in shallow-water environments. Similar distribution of dolomitization within parasequences was described by Lehmann et al. (1998) in rocks of similar age adjacent to the Monterrey Salient. Other dolomitization events also affected these rocks. Burial-related dolomitization events are supported by petrographic textures, fluid inclusion analyses, and results of isotopic analyses in host rock and fractures (Monroy-Santiago et al., 2001; Guzzy-Arredondo et al., 2007; Fischer et al., 2009).

Monroy-Santiago et al. (2001) recognized recrystallization, dedolomitization, and silicification as late diagenetic events in all locations. Recrystallization largely postdated dolomitization, as indicated by corroded dolomite crystals that have lost their original euhedral facets. Silica replacement (silicification) occurred in two forms: (1) late, euhedral quartz crystals in fractures, with inclusions of calcite and dolomite crystals and (2) rare, microcrystalline quartz and chalcedony, selectively replacing dolomitized allochems. Evidence of dedolomitization in the Cupido Formation is documented by aggressive replacement of dolomite by calcite. This late diagenetic event was probably contemporaneous with exhumation and circulation of phreatic waters (Monroy-Santiago et al., 2001).

4. Methodology

Ortega et al. (2006) discussed the problem of lack of explicit accounting for fracture size in previous studies of fracture intensity or spacing (e.g., Bogdonov, 1947; Ladeira and Price, 1981; Narr and Suppe, 1991; Wu and Pollard, 1995; Narr, 1996). Ortega et al. (2006) demonstrated that fracture size and intensity are covariant and proposed a scale-independent approach to fracture intensity and spacing quantification. We adopt their methods for reporting fracture intensity, which they defined for 1D data as the number of fractures encountered per unit length along a sample line oriented perpendicular to a fracture set. We used a fracture-aperture comparator to measure fracture apertures down to ~50 μm by comparing apertures (wall-to-wall width of fracture) with printed lines of calibrated width from 50 μm to 5 mm (Ortega et al., 2006). Fracture intensities were then determined for apertures $\geq$ 0.2 mm from the best-fit aperture-size distribution models for measurements of each set. The 0.2-mm size was chosen for comparison because it is within the midsize range (log scale) for each population. More than 14,200 fracture-aperture values from 42 beds compose the fracture-size database.

Orientation, morphology, and width (kinematic aperture or opening displacement); crosscutting relationships; composition and texture of fracture fill; and mechanical layer thickness were recorded for each fracture set. Mechanical bed thickness, ranging from <10 cm to nearly 2 m, was defined by bed-perpendicular fracture extent (height). At least four fracture sets were identified at each location and have been labeled A, B, C, D, and M from oldest to youngest. Fracture sets with the same label that are from different localities are not necessarily of the same age.

For this study, beds were chosen to represent contrasting sedimentary facies and varying bed thickness and degree of dolomitization (Fig. 3). Fracture-intensity analyses were made for two broadly defined sedimentary facies: mud supported and grain supported. Dolomite content in the rocks studied ranges from 0 to 100%. Most beds are either highly dolomitized or not dolomitized (Fig. 3). Degree of dolomitization was determined in thin sections stained with Alizarin Red, although the relative proportions of dolomite that precipitated in different dolomitization events was not quantified. Sedimentary facies and diagenetic modification were described by Ortega (2002).

Effects of sedimentary and diagenetic factors on fracture intensity were analyzed first by an investigation of simple correlations of each variable and fracture intensity. The number of observations together with the coefficient of determination of weighted regression analyses provided a tool for evaluating relative importance of stratigraphic and diagenetic controls on fracture intensity (Young, 1962). These regressions take into account uncertainties associated with fracture-intensity determinations following the methodology of Jensen et al. (1997). Multivariate analysis allowed the individual contributions of each factor and their cross-correlations to be taken into account (Swan and Sandilands, 1995).

Table 2
Power-law aperture-size distribution parameters for all study locations.

Locality	Bed number	1D-power-law exponent				1D-power-law coefficient			
		Set A	Set B	Set C	Set D	Set A	Set B	Set C	Set D
La Escalera	1	−0.6440	−0.4550			0.0270	0.0270		
	2	−0.7290	−0.9490			0.0250	0.0070		
	3	−0.6850	−0.6100			0.0170	0.0400		
	4			−0.7560			0.0120		
	5B			−0.953[b]				0.0004[b]	
	6A	−0.334[b]		−1.277[b]		0.001[b]		0.00007[b]	
	6B	−0.7070	−0.7710			0.0110	0.0080		
	7	−0.9350	−0.8050			0.0040	0.0100		
	8	−0.8430	−1.0950			0.0150	0.0060		
	9	−0.9120	−0.8210			0.0080	0.0100		
	10		−0.293[b]				−0.003[b]		
	11	−0.9670	0.0040						
	12	−1.374[a]	−1.407[a]			0.003[a]	0.003[a]		
Las Palmas	1	−0.279[c]	−0.6220			0.0043	0.0131		
	2	−1.2650	−1.600[c]			0.0009	0.0000		
	3		−0.1890	−0.5580			0.0096	0.0105	
	4	−0.9470		−0.391[c]		0.0010		0.0035	
	5	−0.7310		−0.9460		0.0017		0.0013	
	6	−1.8520		−2.450[c]		0.0004		0.0001	
	7	−0.5590		−0.4450		0.0036		0.0032	
	8	−0.7490		−0.836[c]		0.0097		0.0013	
	9	−0.4670		−0.5760		0.0181		0.0134	
	10	−0.6060		−0.8470		0.0067		0.0025	
El Chorro	1		−0.5290		−0.445[c]		0.0091		0.0024
	2			−1.9260	−1.2130			0.0005	0.0015
	3	−0.8520	−0.9250			0.0038	0.0034		
	4	−0.5480	−0.9910			0.0035	0.0026		
	5	−0.8630	−0.6650	−0.9920		0.0059	0.0032	0.0014	
	6	−0.8510	−1.3770	−0.563[c]		0.0015	0.0001	0.0012	
	7	−0.6360		−0.533[c]		0.0176		0.0038	
	8	−1.1160		−0.776[c]		0.0011		0.0010	
Iturbide	1	−0.677			−1.045[b]	0.0077			0.0004[b]
	2	−1.123		−1.889[b]		0.0026		0.00006[b]	
	3			−1.31	−0.781			0.0023	0.0023
	4			−0.771	−1.078			0.0031	0.0013
	5	−0.853				0.0049			
	6			−1.101				0.0019	
	7			−0.999				0.0022	
	8				−0.354[d]				0.0284[d]
	9			−1.481	−1.973			0.0005	0.0001
	10	−0.558		−1.845	−1.522	0.011		0.0001	0.0004

[a] Suspect data (recrystallized limestone).
[b] Fewer than 100 fractures measured.
[c] Fewer than 50 fractures measured.
[d] 2D to 1D conversion (Marrett, 1996; Moros, 1999).

5. Fracture descriptions

Fracture orientation data have been illustrated (Figs. 4–6), and scanline statistics have been summarized for all locations (Table 1).

5.1. La Escalera Canyon

Four opening-mode fracture sets are present at La Escalera Canyon (Fig. 4). Sets A and B are the oldest and most abundant and are developed preferentially in dolostone layers. Mutually crosscutting relationships suggest that A and B are contemporaneous. They are distinguished by dip; set A fractures are oblique to bedding, whereas set B are normal to bedding. Fracture set C, normal to bedding and perpendicular to the fold axis, is older than bedding-parallel burial stylolites. Some tectonic stylolites nucleate along set C fracture walls, indicating that set C predates tectonic stylolites. Set D fractures are long, narrow, subparallel to bedding and are kinematically compatible with tectonic stylolites. They are the least abundant set at this locality.

5.2. Las Palmas Canyon

Four opening-mode fracture sets were identified at Las Palmas Canyon (Fig. 4). Sets A and C are the most abundant. Set C trends oblique to the fold axis and dips slightly oblique to bedding. Set C crosscuts sets A and B. Set A fractures strike more northerly than those of set B, and fracture set B dips slightly oblique to bedding, although these sets are likely contemporaneous, given mutually crosscutting relationships. Sets A, B, and C abut, or are crosscut by, bedding-parallel stylolites. A fourth fracture set present at Las Palmas (set M) is characterized by calcite-lined walls and later filled by calcite mud, sometimes containing well-preserved bioclasts. Set M is the youngest fracture set in the area and probably formed after folding occurred.

5.3. El Chorro

Five fracture sets were separated at El Chorro (Fig. 5). Set A forms a higher angle with bedding and is closer to vertical than set B; again, these sets are likely to be contemporaneous. Set C crosscuts sets A and B, is normal to bedding, and is subparallel to the fold

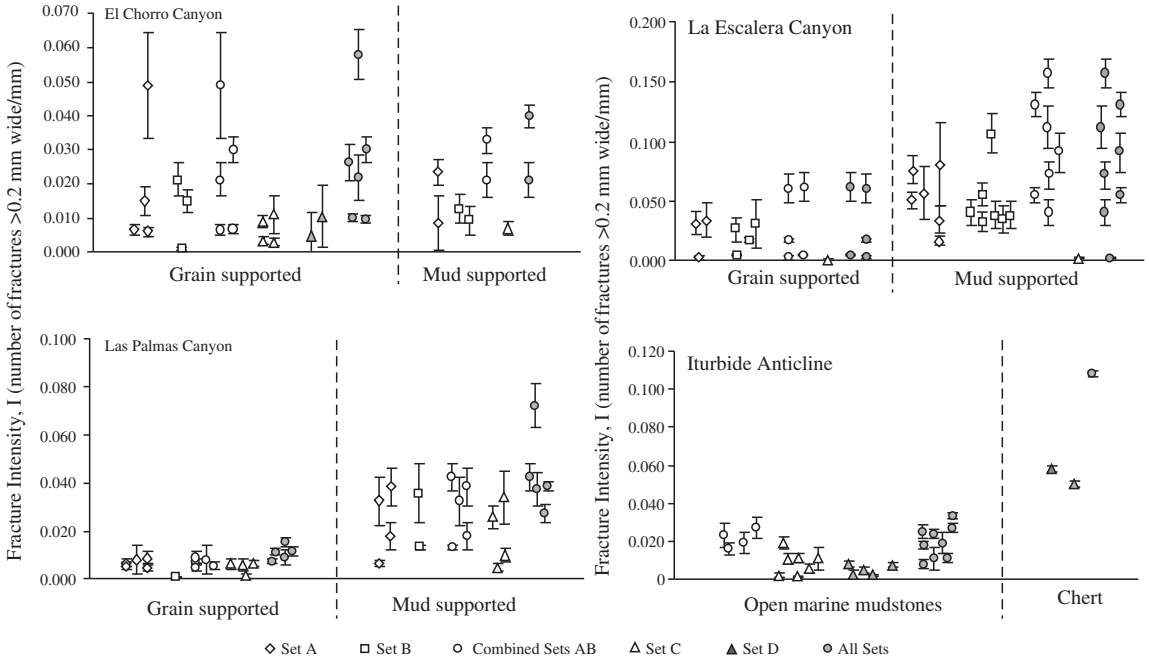

Fig. 8. Sedimentary facies control on fracture intensity.

axis. Sets D1 and D2 are vertical and are interpreted as conjugate shear-vein sets—D1 is oblique to the fold axis and forms a low angle with bedding, whereas D2 is parallel to bedding and is similar to fracture set D at La Escalera Canyon in morphology and geometric relationships.

5.4. Iturbide

Four fracture sets are present at Iturbide (Fig. 6). Fractures are generally long and narrow, but fractures that reach bed boundaries have apertures that locally increase toward the boundary and abruptly terminate there. Fractures are arranged in swarms, commonly with en echelon geometry. Sets A and B predate tectonic stylolites and crosscut one another, with systematic small offsets suggesting synchronous timing and conjugate origin. The shear offsets are smaller than fracture apertures, suggesting dominantly opening-mode movement. Set C is oblique to the fold axis and is older than burial stylolites. Set D, orthogonal to bedding and to the fold axis, forms a high angle with tectonic stylolites and consequently is kinematically compatible with them.

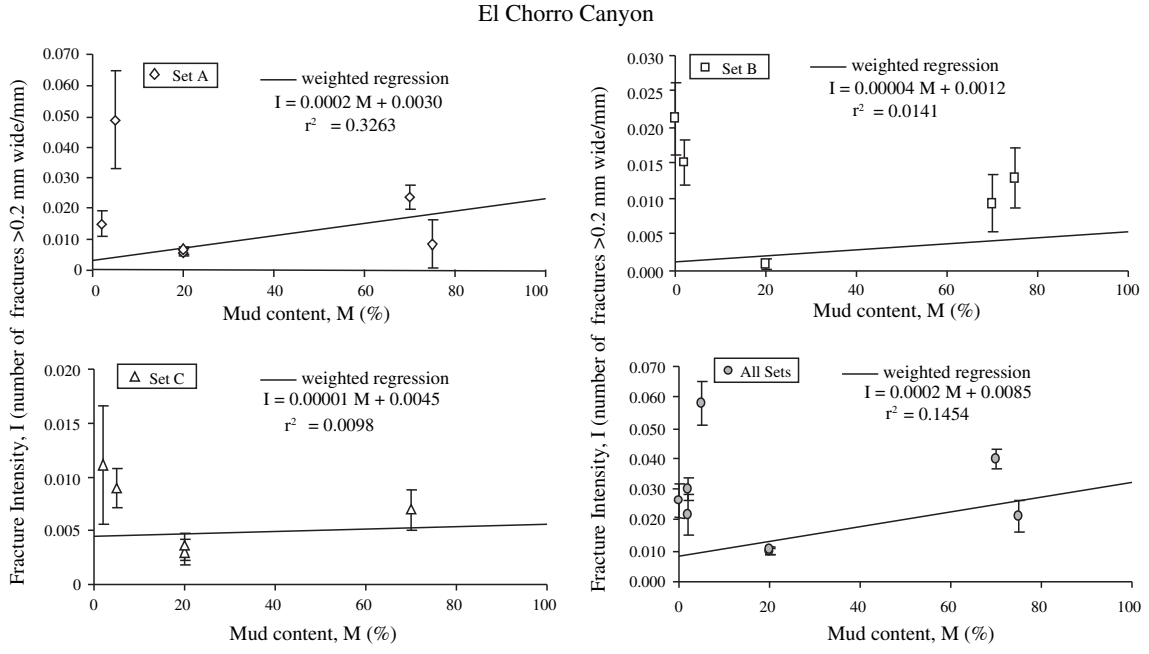

Fig. 9. Normalized fracture intensity and mud content, El Chorro Canyon. Probability of obtaining similar coefficients of determination between two uncorrelated variables is more than 10%.

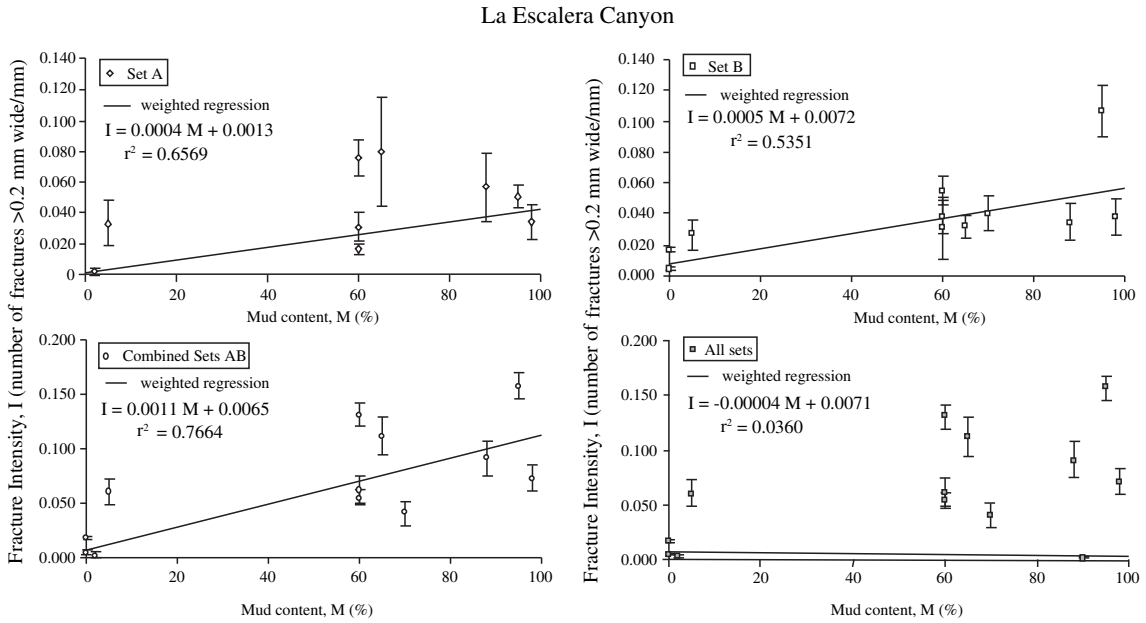

Fig. 10. Normalized fracture intensity and mud content, La Escalera Canyon. The coefficients of determination for regressions vary from $r^2 = 0.5351$ for set B to $r^2 = 0.7664$ for sets A and B combined, suggesting that there is less than a 2% chance that these variables are uncorrelated. The slope of the regression lines suggests that mud content can produce a variation of fracture intensity from 0.04 to 0.12 fractures/mm, in fractures with aperture greater than 0.2 mm.

5.5. Petrography

Petrographic analyses of samples from the 43 carbonate beds studied allowed a comparison with the paragenetic sequence established by Monroy-Santiago et al. (2001) (Fig. 7). Petrography was described by Ortega (2002), and his findings relevant to this study are summarized here. Fractures are partly or completely sealed, and cements include calcite, dolomite, and quartz. Fractures in dolostones, lined by euhedral dolomite crystals, contain dolomite bridges from wall to wall, suggesting that dolomite was the first mineral phase filling these fractures. Multiple dolomite bridges adjacent to one another give a fibrous texture to the fracture fill, with saw-tooth contacts between the fibers. Ramsay (1980) described similar fibrous veins and interpreted them as indicative of cementation synchronous with fracture opening. Calcite cement precipitated after dolomite precipitated, filling the remaining pore space in fractures. Dolomite is synkinematic, calcite is post-kinematic (Laubach, 2003; Gale et al., 2010), and dolomite-lined

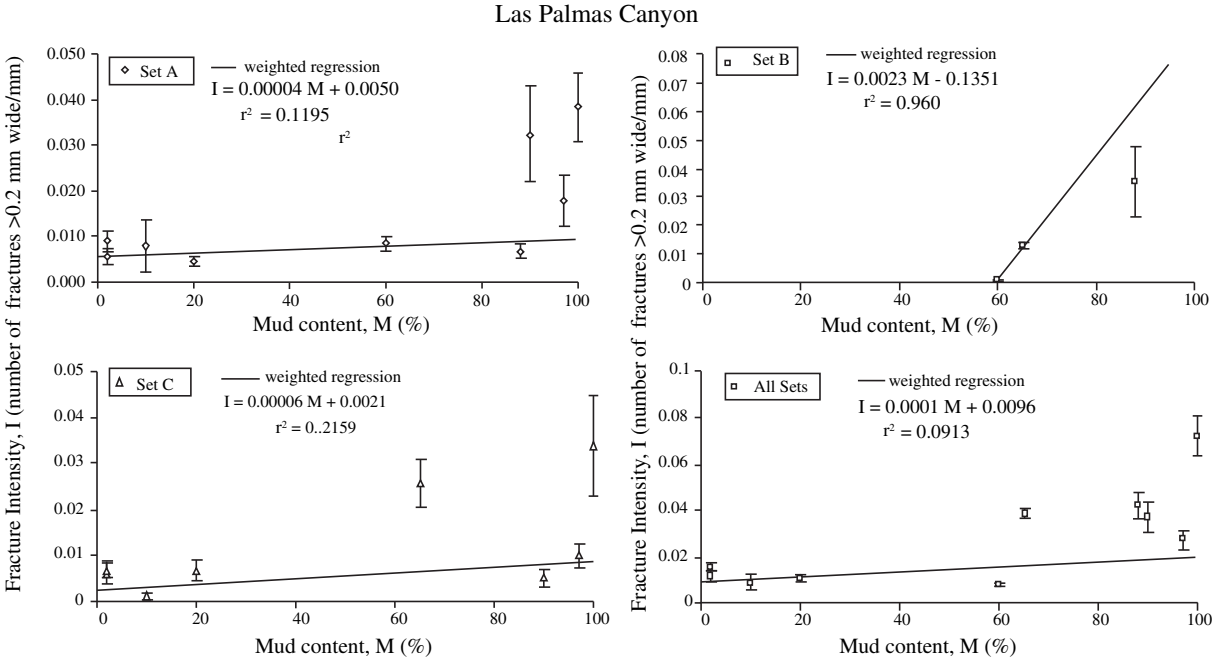

Fig. 11. Normalized fracture intensity and mud content, Las Palmas Canyon. The coefficients of determination for these weighted regressions show a large range: $r^2 = 0.1195$ for set A, $r^2 = 0.2159$ for set C, $r^2 = 0.0913$ for all sets combined. Probability of obtaining similar coefficients of determination between two uncorrelated variables is >10%.

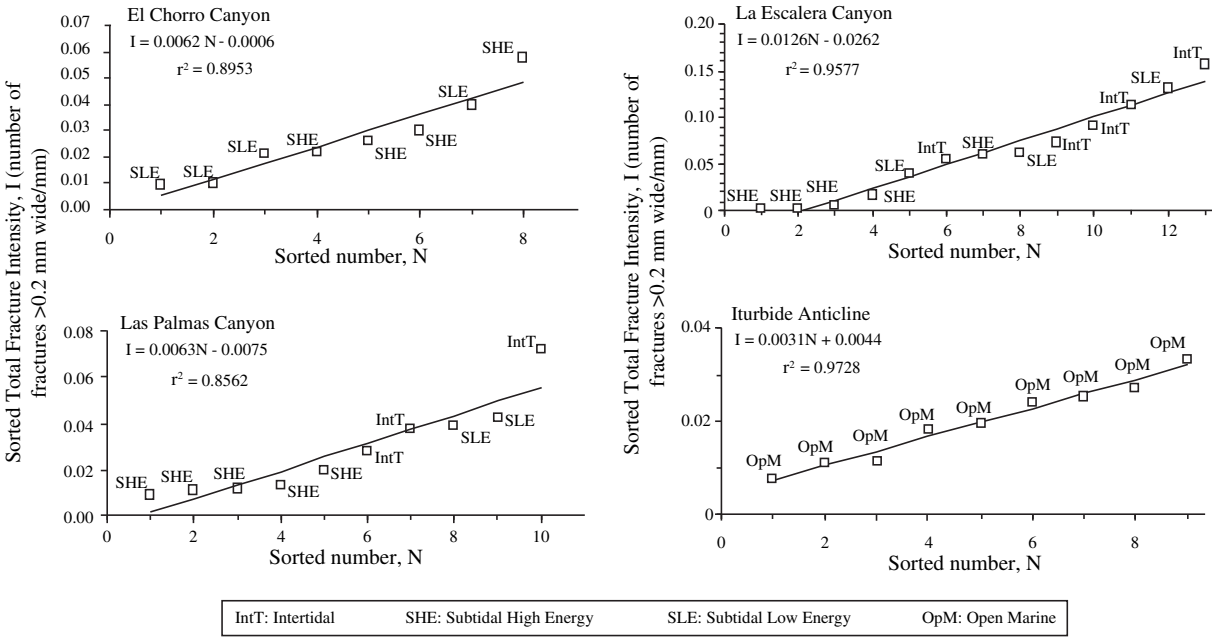

Fig. 12. Total normalized fracture intensity and interpreted environment of deposition. Fracture intensity was sorted from lowest to highest, and beds numbered sequentially.

fractures most likely contained significant and persistent open pore space until fractures were sealed by late calcite, possibly late in the Cupido Formation's burial history (Monroy-Santiago et al., 2001). Recrystallization did not occur in all limestone beds, but where present, it blurred the contrast between mineral fill in older fractures and matrix and obscured fractures having apertures smaller than the mean recrystallized grain size. Only a few grainstones and boundstones recrystallized to sparry calcite. In these cases, fractures with apertures < 0.1 mm can be indistinguishable from matrix. Dedolomitization and silicification affected dolomite and calcite cements in fractures and matrix.

6. Normalized fracture-intensity results and statistical analysis of controls on fracture intensity

Aperture-size data for each scanline were plotted as cumulative–frequency plots, and best-fit size distribution equations were defined. Power-law exponents and coefficients obtained from the equations are summarized in Table 2. We used these equations to obtain normalized fracture-intensity numbers and plotted them (Figs. 8–23). The plots show variation in intensity with a series of parameters: facies type, mud content, depositional environment, bed thickness, and dolomite content.

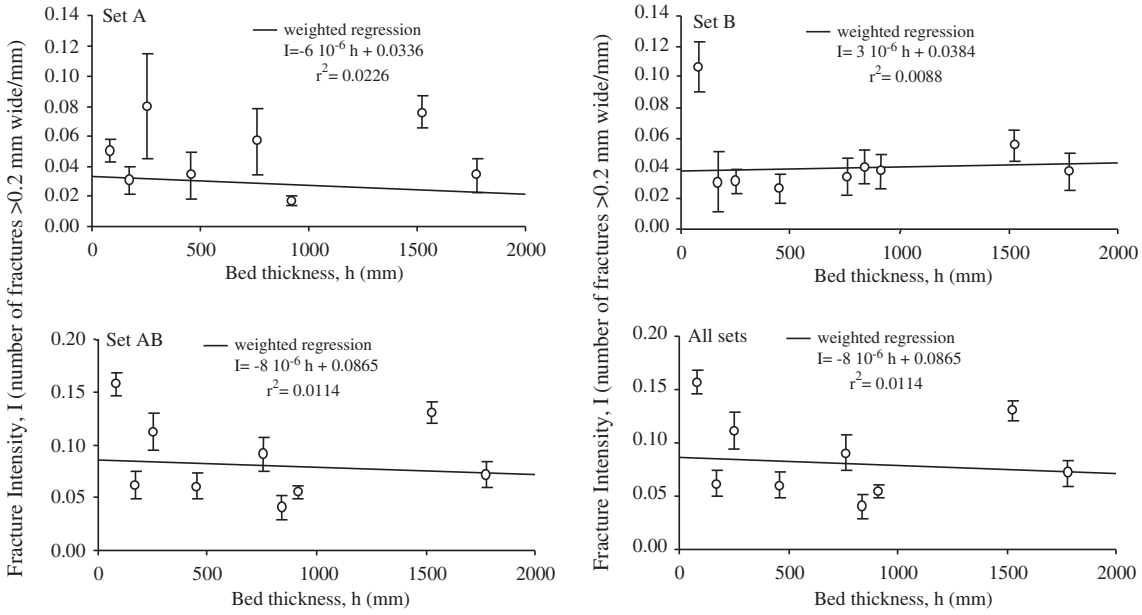

Fig. 13. Bed thickness control on fracture intensity in dolostone beds (>50% dolomite content), La Escalera Canyon. The coefficient of determination for set A, based on data from 8 beds, is $r^2 = 0.0226$, and the coefficient of determination for set B, based on 9 beds, is $r^2 = 0.0088$. The coefficient of determination to the combination of sets A and B is also very close to zero ($r^2 = 0.0114$).

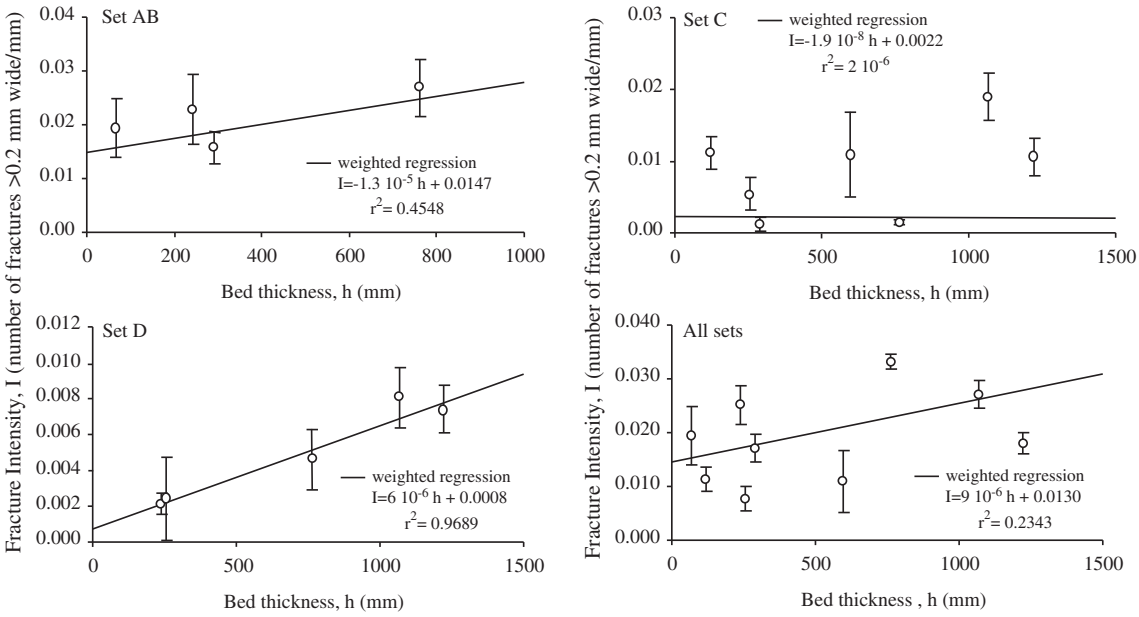

Fig. 14. Bed thickness control on fracture intensity, open-marine mudstones, Iturbide Anticline. Weighted regression to fracture intensity for all sets yields a low coefficient of determination ($r^2 = 0.2343$) suggesting that fracture intensity increases with bed thickness, similar to the relationship obtained for fracture sets AB and D, although there is more than 10% probability of obtaining this degree of correlation for similar number of data points between uncorrelated variables.

6.1. Sedimentary facies control on fracture intensity

Facies were interpreted by thin-section analysis of rock composition, texture, biologic content, energy level during deposition (following Dunham, 1962), and position of the bed within stratigraphic cycles. Intensities were compared for mud-supported vs. grain-supported facies at the different localities (Fig. 8), and then intensities were analyzed against mud content by set for El Chorro, La Escalera, and Las Palmas (Figs. 9–11).

6.1.1. El Chorro

Fracture intensities in grain-supported and mud-supported beds overlap considerably (Fig. 8). Weighted regressions suggest that fracture intensity of each set increases with an increase in mud content in the rock but that the correlation is weak (Fig. 9). Most beds studied are grain supported; only two layers have >50% mud content.

6.1.2. La Escalera

Fracture intensity and mud content have a modest, positive correlation in Sets A, B, and AB combined (Fig. 10). Fracture set C intensity was measured in only two beds with low fracture intensity—a grain-supported bed and a mud-supported subtidal facies layer. If these results are included in the plot for all sets (Fig. 10), then the weighted regressions indicate no correlation between mud content and fracture intensity.

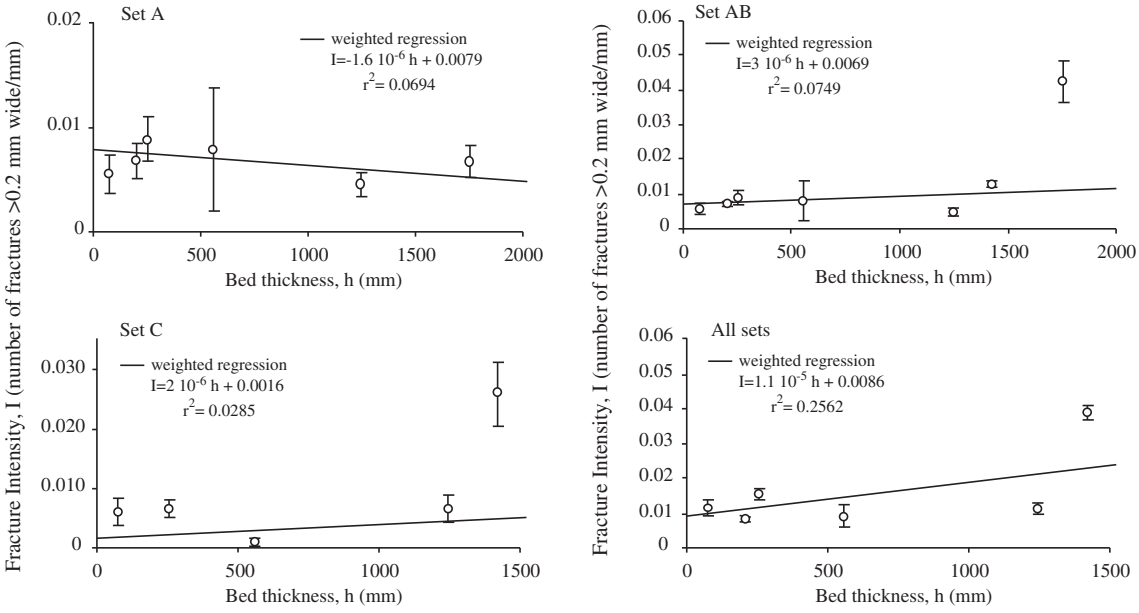

Fig. 15. Normalized fracture intensity and bed thickness, limestones (<50% dolomite content), Las Palmas Canyon.

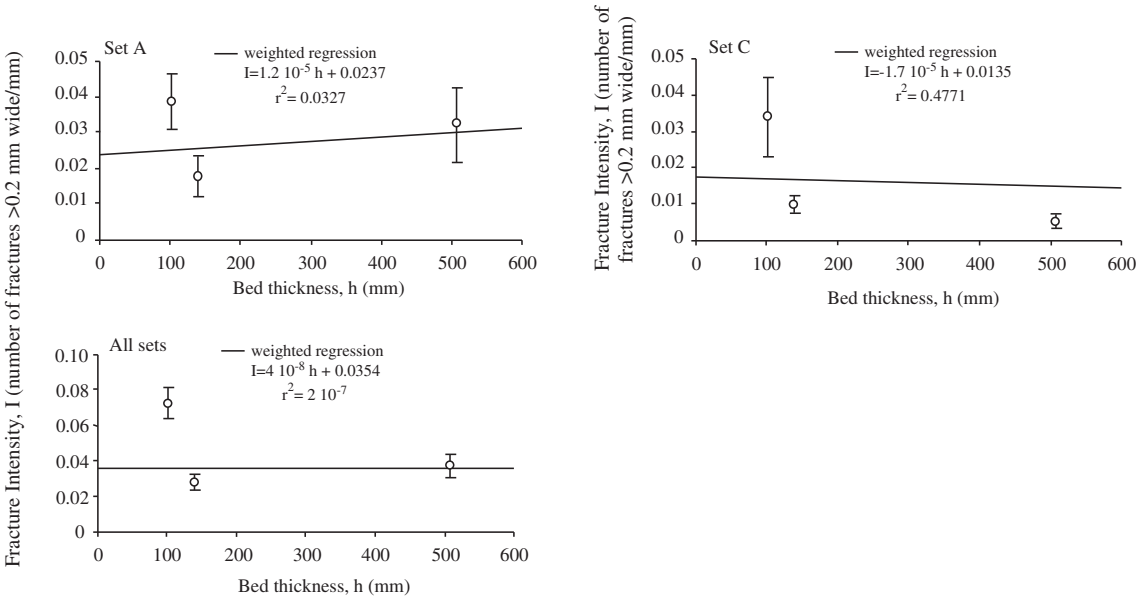

Fig. 16. Normalized fracture intensity and bed thickness, dolostones (>50% dolomite content), Las Palmas Canyon.

6.1.3. Las Palmas

Mud-supported beds show generally higher fracture intensities than grain-supported beds (Fig. 8). Linear regressions of fracture intensity vs. mud content indicate a positive correlation between these two parameters (Fig. 11), consistent with results from El Chorro and La Escalera.

6.1.4. Iturbide

Fracture intensity in chert nodules is as much as twice that in mudstone beds (Fig. 8). Fracture intensities for individual sets in Iturbide mudstones are, on average, lower than fracture intensities observed in shallow-water, mud-supported rocks of the Cupido Formation.

6.2. Sedimentary environment of deposition control on fracture intensity

Fracture intensity was sorted from lowest to highest, and bed numbers were assigned starting with 1 for lowest intensity. A regression line to the cross-plot of fracture intensity vs. bed number was then allowed to represent an upper limit of correlation for the population (Fig. 12). Each data point was labeled with the interpreted environment of deposition, allowing an assessment of sedimentary environment control on fracture intensity. At El Chorro, the highest fracture intensities are associated with high-energy layers and one subtidal, low-energy wackestone. Also at El Chorro, the lowest fracture intensities occur in subtidal, low-energy deposits. At Las Palmas, lower fracture intensity is associated with high-energy, subtidal environments, typically grainstones, packstones, and rudist banks with grain-supported matrix. Similar results were obtained for La Escalera Canyon, although exceptions occur. For example, a dolomitized ooid grainstone, interpreted as a shoal deposit in a high-energy, subtidal environment, has higher fracture intensity than other intertidal or subtidal, low-energy deposits. The range of variation of fracture intensity in Iturbide mudstones is small, suggesting that all mudstone beds had similar resistance to brittle failure. Sedimentary environment considerations at Iturbide are trivial because all beds studied were deposited in an open-marine environment.

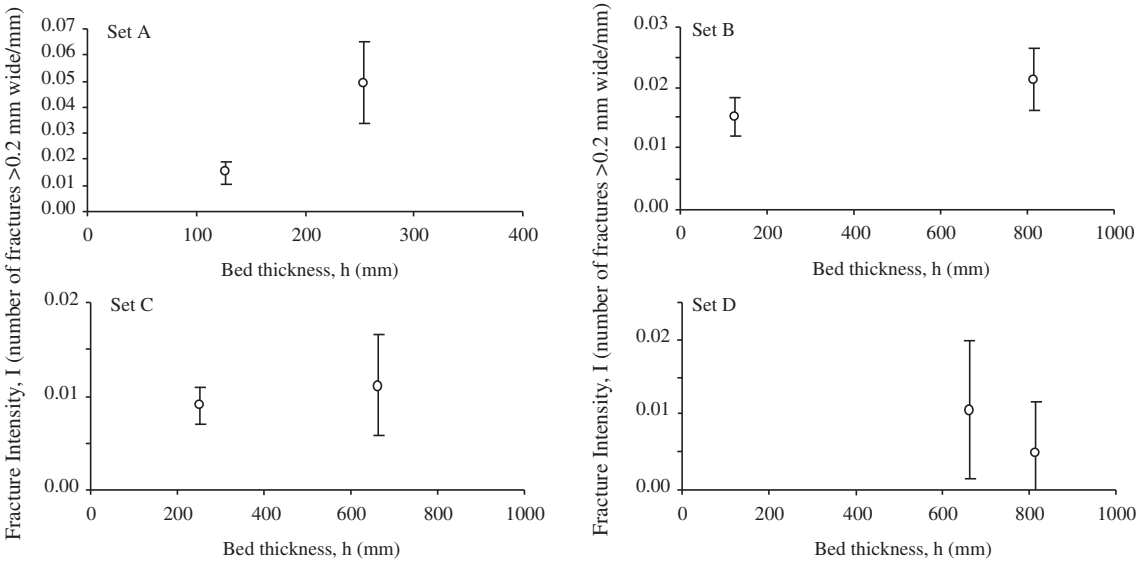

Fig. 17. Normalized fracture intensity and bed thickness, grainstones, El Chorro Canyon.

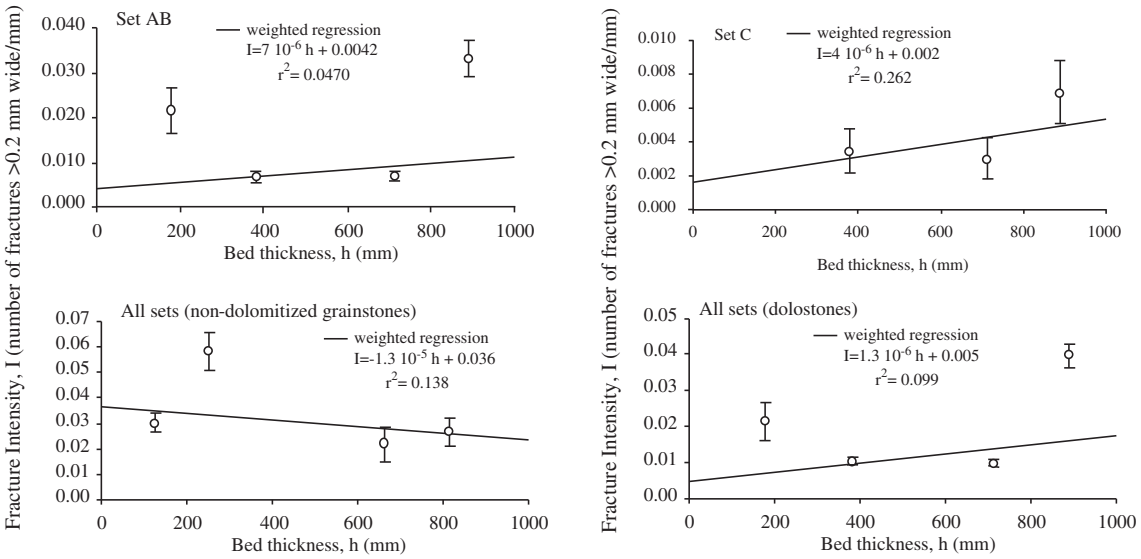

Fig. 18. Normalized fracture intensity and bed thickness, dolostones (>70% dolomite content), El Chorro Canyon.

6.3. Bed-thickness control on fracture intensity

Ideally, comparison of fracture intensities would be made in beds having different thicknesses, at the same locality, and similar mechanical properties at the time of fracturing. Although we studied fracture intensity in more than 40 beds from Cupido and Tamaulipas Inferior Formations, finding a representative subset of beds that meets all these requirements was difficult. Because the sedimentary facies does not have a first-order control on fracture intensity, we analyzed bed thickness vs. fracture-intensity relationships in all limestone beds from Las Palmas as one group, and the remaining three dolostones as a separate group. Similarly, at El Chorro, limestones and dolostones were analyzed as two separate groups.

6.3.1. La Escalera

Weighted regressions for dolostones suggest that there is little to no correlation between bed thickness and fracture intensity at La Escalera Canyon (Fig. 13). The coefficient of determination for least-squares regression to total fracture intensity is close to zero. Weighted regression lines for individual fracture sets also yield low coefficients of determination. Results for set C are not shown because this set is sufficiently developed in only two limestone beds and regression to only two points is trivial.

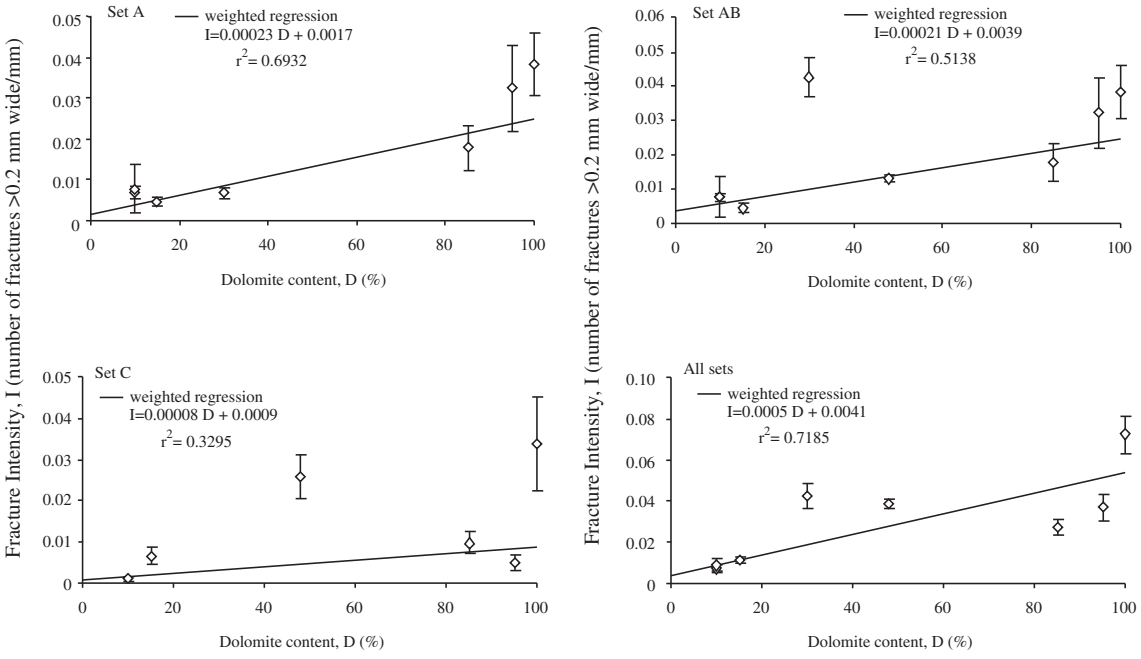

Fig. 19. Normalized fracture intensity and dolomite content, Las Palmas Canyon. The coefficient of determination for a linear weighted regression to total fracture intensity per bed is high ($r^2 = 0.72$), suggesting that there is less than 1% probability of obtaining this degree of correlation from spurious data.

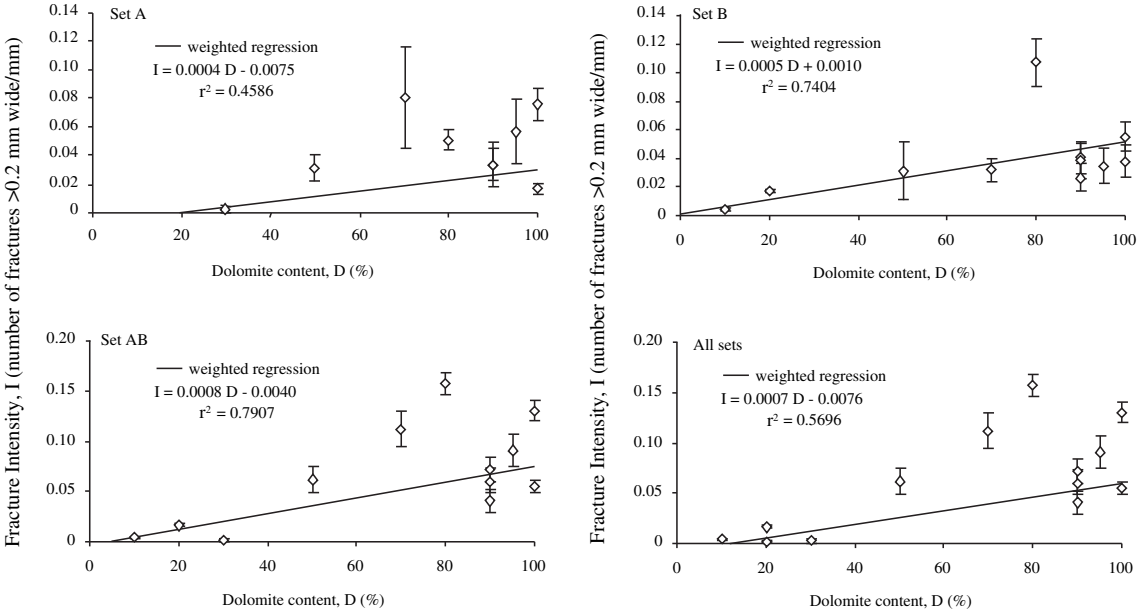

Fig. 20. Normalized fracture intensity and dolomite content, La Escalera Canyon. The coefficient of determination for independent sets A (9 beds) and B (11 beds) at La Escalera is $r^2 = 0.4586$ and $r^2 = 0.7404$, respectively. There is less than a 5% probability of obtaining the degree of correlation found for set A from uncorrelated variables, and the probability is less than a fraction of a percent for set B.

6.3.2. Iturbide

Fracture intensity at Iturbide is inconsistently correlated with bed thickness (Fig. 14). Weighted linear regression suggests an increase of fracture intensity with an increase in bed thickness. The coefficient of determination for fracture set C in six beds is close to zero, suggesting no correlation between bed thickness and fracture intensity. At Iturbide, tectonic stylolites developed locally along fracture walls, reducing the apertures of some fractures in sets A, B, and C and thus preventing measurement of the original fracture apertures. Results from set D, unaffected by tectonic stylolites, produce the strongest positive correlation between fracture intensity and bed thickness.

6.3.3. Las Palmas

Bed-thickness–fracture-intensity relationships in the Las Palmas dataset are inconsistent (Fig. 15). Weighted regressions to individual and combined fractured sets are characterized by low statistical reliability, suggesting either no or weak correlation (both positive and negative) between bed thickness and fracture intensity (Fig. 16).

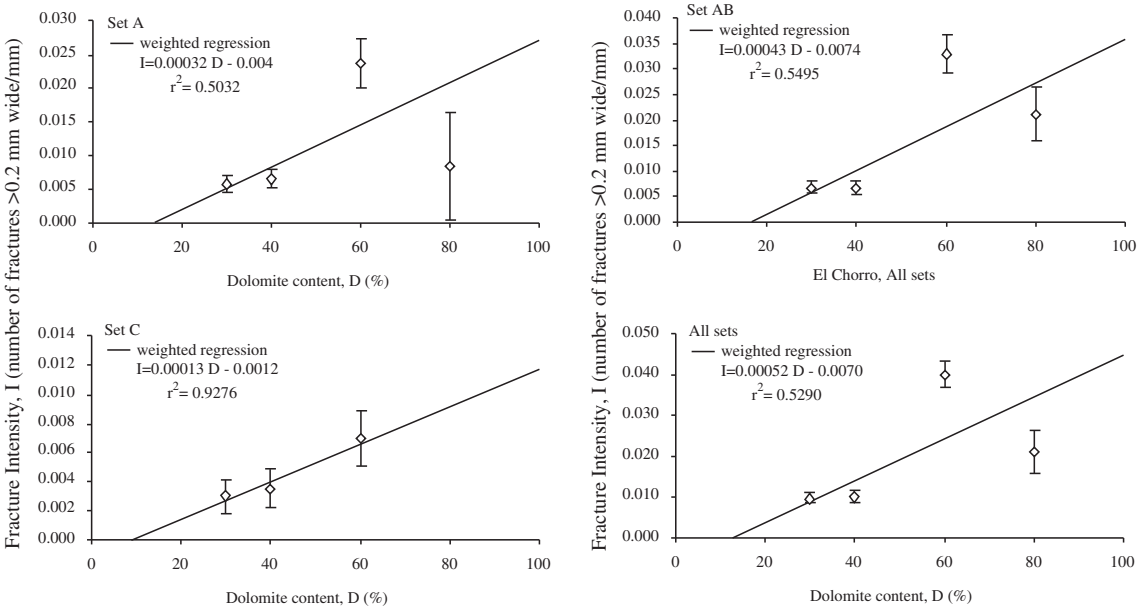

Fig. 21. Normalized fracture intensity and dolomite content, El Chorro Canyon. The coefficient of determination is moderately high and similar for set A ($r^2 = 0.5032$), combined sets AB ($r^2 = 0.5495$), and total intensity combining all sets ($r^2 = 0.5290$). Weighted regression to only three points from set C yields a very high coefficient of determination ($r^2 = 0.9276$), however, this value is not high enough to indicate less than a 10% probability of correlation by chance.

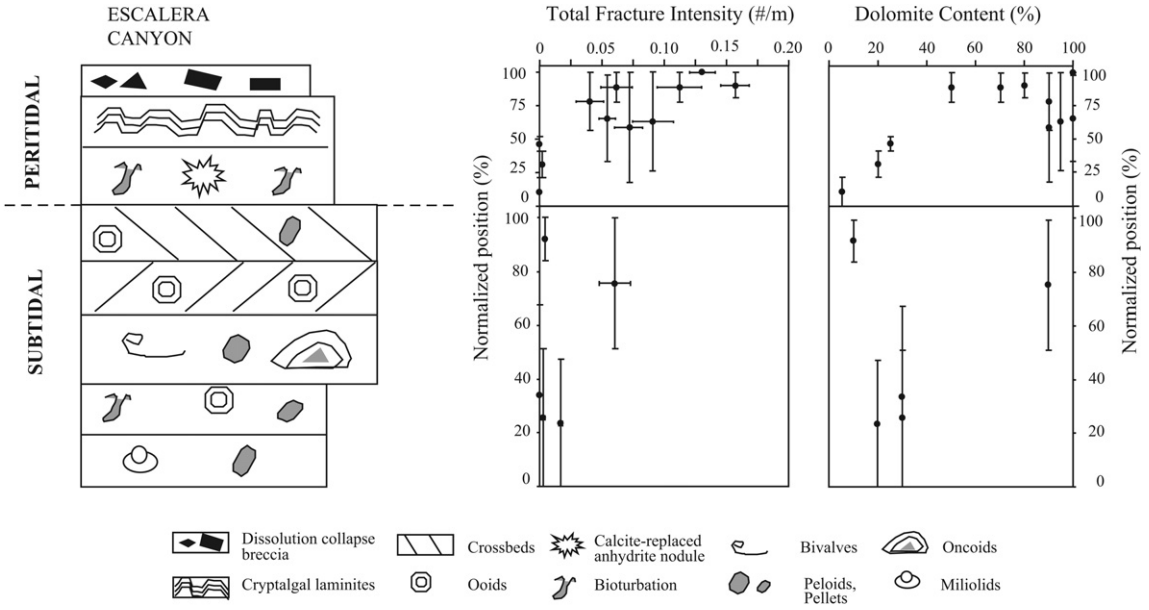

Fig. 22. Schematic distribution of fracture intensity and degree of dolomitization in peritidal and subtidal parasequences at La Escalera Canyon.

6.3.4. El Chorro

El Chorro beds can be separated into limestones (Fig. 17) and dolostones (Fig. 18). Most data suggest no relationship between bed thickness and fracture intensity. The second-most-common relationship is a positive correlation and the least common is an inverse relationship.

6.4. Dolomitization control on fracture intensity

Consistency in the relationship between dolomite content and fracture intensity and moderate to high coefficients of determination indicates that dolomite content and fracture intensity are systematically related. This relationship, and the presence of syn-kinematic dolomite in the fractures, suggests that fracturing and dolomitization are linked processes.

6.4.1. Las Palmas

There is a positive correlation between normalized fracture intensity and dolomite content at Las Palmas (Fig. 19). Linear regressions for individual set A, combined sets AB, and set C at Las Palmas Canyon also suggest a positive correlation between fracture intensity and dolomite content.

6.4.2. La Escalera

La Escalera data also suggest a positive correlation between fracture intensity and dolomite content (Fig. 20). Coefficients of determination from data at La Escalera are similar to those from Las Palmas. Different degrees of dolomitization are present at Las Palmas Canyon, although at La Escalera most beds are highly dolomitized, and control for weakly dolomitized beds is only sparse. Petrographic work on La Escalera and Las Palmas samples suggests

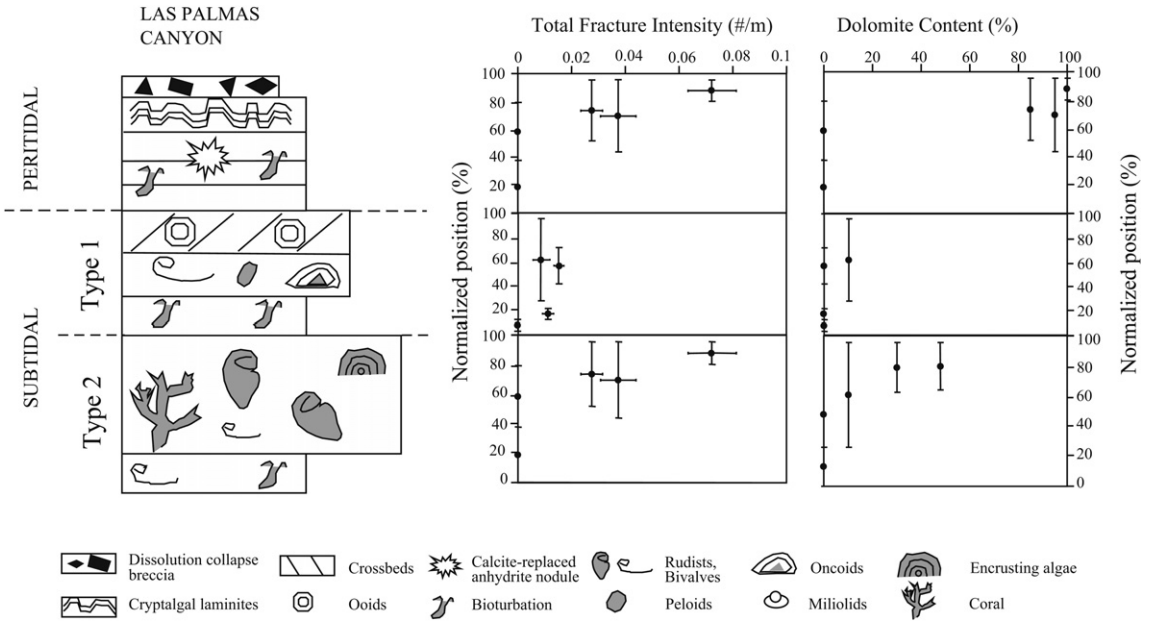

Fig. 23. Schematic distribution of fracture intensity and dolomite distribution in peritidal and subtidal parasequences at Las Palmas Canyon.

Table 3
Summary output of multiple linear-regression analysis for combined fracture sets A, B and C, fracture intensity and stratigraphic variables.

Regression statistics						
Multiple *R*						0.682644663
R square						0.466003736
Adjusted *R* square						0.404975591
Standard error						0.027759922
Observations						40
	df	SS	MS		*F*	Significance *F*
Regression	4	0.02353725	0.005884		7.635882	0.000156164
Residual	35	0.026971465	0.000771			
Total	39	0.050508714				
	Coefficients	Standard error	*t* Stat	*P*-value	Lower 95%	Upper 95%
Intercept	−0.02881704	0.015525799	−1.85607	0.071878	−0.060336131	0.002702
Dolomite	0.000382674	0.000133816	2.859702	0.007102	0.000111013	0.000654
Mud	0.000183544	0.000113896	1.611499	0.116054	−4.76784E − 05	0.000415
Position	0.000653642	0.000235163	2.779525	0.008699	0.000176235	0.001131
Thickness	−3.6505E − 06	9.60945E − 06	−0.37988	0.706328	−2.31587E − 05	1.59E − 05

that some dolomite postdates the fractures. This may explain the scatter of data in both localities.

6.4.3. El Chorro

Dolomite content at El Chorro is >30% in four beds studied and is very low in the other four. Dolomite content vs. fracture-intensity analyses are consistent with results obtained in Las Palmas and La Escalera, suggesting a positive correlation between fracture intensity and dolomite content (Fig. 21).

6.5. Cyclostratigraphic control on fracture intensity

Fracture intensity in beds generally increases toward the top of the parasequences in the peritidal facies (Figs. 22 and 23). Because dolomitized cycle tops dominate the section, there is an impression of a correlation between stratigraphic position and fracture intensity. Some subtidal cycles capped by grainstone shoals or bivalve banks do not, however, show an increase of fracture intensity toward the top of the parasequence. For example, in the middle part of the Las Palmas section, a succession of subtidal cycles is capped by limestone grainstone shoals and/or rudist bioherms that are mostly barren of fractures. Moreover, subtidal cycles with no fractured layers lack dolostone caps. We conclude that it is the degree of dolomitization that is important rather than position in the cycle.

7. Correlation between stratigraphic variables

In the previous section, fracture intensity was the dependent variable, whereas dolomite content, sedimentary facies, position of the bed in the stratigraphic cycle, and bed thickness were independent variables. In this section, degree of correlation between independent variables is analyzed. Correlation among independent variables indicates a need for multivariate techniques in order for the data to be studied (Swan and Sandilands, 1995). In a preliminary bivariate analysis, dolomite content, normalized position in the parasequence, environment of deposition, and mud content show moderate correlation. There is no correlation between bed thickness and the other variables.

Multiple-regression analysis of 40 beds yields results similar to those obtained from bivariate analyses. Four variables were included in the multivariate analysis: dolomite content, mud content, position of bed in the stratigraphic cycle, and bed thickness. In multiple linear-regression analysis, variables that are known to have little effect on fracture intensity—for example, bed thickness—should be excluded. Because the bed-thickness effect on fracture intensity has been an important paradigm, however, this variable was included in the analysis. Fracture sets A, B, and C most likely formed before folding, allowing them to be studied as a group. Set D and set M fractures are excluded because they formed by a mechanism different from that of sets A, B, and C. Results of multivariate analysis of combined sets A, B, and C are shown in Table 3.

Multiple linear-regression coefficients of determination suggest a reliable correlation between variables considered and fracture intensity. *F*-tests suggest high confidence in the coefficient of determination, with negligible (<0.1%) probability of similar degree of correlation by chance. Dolomite content is the most important factor influencing fracture intensity and contributes nearly 60% of the effect on fracture intensity. *T*-tests on dolomite content suggest >9% confidence in determination of this coefficient. Normalized position in the stratigraphic cycle is also an important parameter determining fracture intensity. *T*-tests suggest a confidence level of 93%. The *F* value allows rejection of the null hypothesis (no correlation), with <1% probability of obtaining these coefficients of determination by chance. *T*-tests suggest that correlation between fracture intensity, dolomite content, and position of bed in a cycle is statistically significant, with >95% reliability in the coefficients of determination. Mud-content and bed-thickness *T*-test statistics suggest, respectively, poor and negligible correlations with fracture intensity. Multiple-regression analysis for combined sets AB and C separately and for total fracture intensity at La Escalera yielded results similar to those reported in Table 3, although degree of correlation is lower, and the coefficients are less reliable.

8. Discussion

The dominant control of fracture intensity in the carbonate platform studied is degree of dolomitization, which is linked partly to stratigraphic position because the tops of peritidal parasequences are preferentially dolomitized. However, the link is not universal because dolomitization fronts can extend to include subtidal facies (Morrow, 1982) and subtidal parasequences with no peritidal caps may lack dolomitized layers.

Fracture intensity shows no significant correlation with bed thickness in most cases. In a few cases where there is weak correlation, intensity generally *increases* with an increase in bed thickness. This increase is opposite to the expected behavior (Huang and Angelier, 1989; Ji and Saruwatari, 1998; Nelson, 2001, and references therein), in which fracture intensity is expected to

decrease (fracture spacing increases) with increasing bed thickness. Our results demonstrate that dolomite content rather than bed thickness is the dominant control over fracture intensity or spacing, highlighting the potential importance of diagenetic and mechanical-property history in governing fracture patterns (Laubach et al., 2009). Early dolomitization made parasequence tops more brittle than surrounding mud-supported subtidal facies, including possibly unconsolidated grainstones. For example, adjacent non-dolomitized beds could deform by distributed grain-boundary sliding, whereas dolomitized layers were more cemented and deformed brittly. Subsequent dolomitization at greater burial depth may have been enhanced in beds containing previously formed dolomite crystals that could act as nuclei for precipitation. Differences in volume, distribution, and timing of early and late dolomite may account for the range of observed fracture intensities within dolostones.

9. Conclusions

A study of normalized fracture-intensity variations with sedimentary facies, bed thickness, and degree of dolomitization in Cupido and Tamaulipas Formations suggests that degree of dolomitization is the most robust predictor of fracture abundance. These relationships were documented for individual and combined fracture sets in four different localities using bivariate weighted regressions and multivariate methods. Analyses of fracture textures show that dolomite precipitation and fracturing occurred, at least partly, synchronously in these rocks. Early dolomitization possibly controlled location of fracture initiation under shallow burial conditions, with fracture opening continuing at greater depth, as recorded by crack-seal textures. Degree of dolomitization is related partly to stratigraphic positions of beds within fifth-order sequence-stratigraphic cycles. A sequence-stratigraphic-diagenetic-fracturing model of fracture intensity has potential use in fracture-system prediction in similar carbonate successions. For the outcrops studied, the classic bed-thickness–fracture-spacing relationship—a long-standing paradigm in structural geology—does not apply.

Acknowledgements

This study was partly supported by the National Science Foundation Grant EAR-9614582, the Texas Advanced Research Program Grant 003658-011, and the industrial associates of the Fracture Research and Application Consortium: Anadarko, Bill Barrett Corp., BG Group, ChevronTexaco, Conoco Inc., Devon Energy Corporation, Ecopetrol, EnCana, EOG Resources, Huber, Instituto Mexicano del Petroleo, Japan National Oil Corp., Lariat Petroleum Inc., Marathon Oil, Petroleos Mexicanos Exploracion y Produccion, Petroleos de Venezuela, Petrobras, Repsol-YPFMaxus, Saudi Aramco, Shell, Schlumberger, Tom Brown, TotalFinaElf, Williams Exploration & Production. Faustino Monroy-Santiago, Steve Laubach, Jon Olson, John Hooker and Bob Goldhammer contributed valuable discussion. Lana Dietrich edited the manuscript. Andrea Billi and Gustavo Murillo-Muñeton and the special issue editor Steve Laubach gave thorough and helpful reviews.

References

Agosta, F., Tondi, E. (Eds.), 2009. Deformation in Carbonates. Journal of Structural Geology 31 (special issue).

Antonellini, M., Mollema, P.N., 2000. A natural analog for a fractured and faulted reservoir in dolomite: Triassic Sella Group, Northern Italy. AAPG Bulletin 84, 314–344.

Bai, T., Pollard, D.D., 2000. Fracture spacing in layered rocks: a new explanation based on the stress transition. Journal of Structural Geology 22, 43–57.

Bogdonov, A.A., 1947. The intensity of cleavage as related to the thickness of beds. Soviet Geology 16, 102–104.

Camerlo, R.H., 1998. Geometric and Kinematic Evolution of Detachment Folds, Monterrey Salient, Sierra Madre Oriental, Mexico. The University of Texas at Austin, Master's thesis, 399 p.

Casey, M., Butler, R.W.H., 2004. Modelling approaches to understanding fold development: implications for hydrocarbon reservoirs. Marine and Petroleum Geology 21, 933–946.

Conklin, J., Moore, C., 1977. Environmental analysis of the Lower Cretaceous Cupido Formation, Northeast Mexico. Report of Investigations No. 89. In: Bebout, D.G., Loucks, R.G. (Eds.), Cretaceous Carbonates of Texas and Mexico. The University of Texas at Austin, Bureau of Economic Geology, pp. 302–323.

Corbett, K., Friedman, M., Spang, J., 1987. Fracture development and mechanical stratigraphy of Austin Chalk. Texas. AAPG Bulletin 71, 17–28.

Das Gupta, U., 1978. A Study of Fractured Reservoir Rocks, with Special Reference to Mississippian Carbonate Rocks of Southwest Alberta. University of Toronto, Ph.D. thesis, 261 p.

Dunham, R.J., 1962. Classification of carbonate rocks according to depositional texture. In: W.E.Ham (Ed.), Classification of Carbonate Rocks. American Association of Petroleum Geologists, pp. 108–121. Memoir 1.

Ferrill, D.A., Morris, A.P., 2008. Fault zone deformation controlled by carbonate mechanical stratigraphy, Balcones fault system. Texas. AAPG Bulletin 92, 359–380.

Fischer, M.P., Gross, M.R., Engelder, T., Greenfield, R.J., 1995. Finite element analysis of the stress distribution around a pressurized crack in a layer elastic medium: implications for the spacing of fluid-driven joints in bedded sedimentary rock. Tectonophysics 247, 49–64.

Fischer, M.P., Higuera-Díaz, I.C., Evans, M.A., Perry, E.C., Lefticariu, L., 2009. Fracture-controlled paleohydrology in a map-scale detachment fold: insights from the analysis of fluid inclusions in calcite and quartz veins. Journal of Structural Geology 31, 1490–1510.

Fischer, M.P., Jackson, P.B., 1999. Stratigraphic controls on deformation patterns in fault-related folds: a detachment fold example from the Sierra Madre Oriental, Northeast Mexico. Journal of Structural Geology 21, 613–633.

Gale, J.F.W., Lander, R.H., Reed, R.M., Laubach, S.E., 2010. Modeling fracture porosity evolution in dolostone. Journal of Structural Geology 32, 1201–1211.

Gillespie, P.A., Howard, C.B., Walsh, J.J., Watterson, J., 1993. Measurement and characterization of spatial distributions of fractures. Tectonophysics 226, 113–141.

Gillespie, P.A., Johnston, J.D., Loriga, M.A., McCaffrey, K.L.W., Walsh, J.J., Watterson, J., 1999. Influence of layering on vein systematics in line samples. In: McCaffrey, K.J.W., Lonergan, L., Wilkinson, J.J. (Eds.), Fractures, Fluid Flow, and Mineralization. Geological Society of London, 155. Special Publication, pp. 35–56.

Gillespie, P.A., Walsh, J.J., Watterson, J., Bonson, C.G., Manzocchi, T., 2001. Scaling relationships of joint and vein arrays from The Burren, Co. Clare, Ireland. In: Dunne, W.M., Stewart, I.S., Turner, J.P. (Eds.), Paul Hancock Memorial Issue. Journal of Structural Geology, 23, pp. 183–201.

Goldhammer, R.K., Lehman, P.J., Todd, R.G., Wilson, J.L., Ward, W.C., Johnson, C.R., 1991. Sequence Stratigraphy and Cyclostratigraphy of the Mesozoic of the Sierra Oriental, Northeast Mexico. Society of Economic Paleontologists and Mineralogists, GulfCoast Section, 85 p.

Goldhammer, R.K., 1999. Mesozoic sequence stratigraphy and paleogeographic evolution of northeastern Mexico. In: Mesozoic Sedimentary and Tectonic History of North-Central, 340. Geological Society of America, Mexico, pp. 1–59. Special Paper No.

Guzzy-Arredondo, G.S., Murillo-Muñetón, G., Morán-Zenteno, D.J., Grajales-Nishimura, J.M., Martínez-Ibarra, R., Schaaf, P.E.G., 2007. High-temperature dolomite in the Lower Cretaceous Cupido Formation, Bustamante Canyon, northeast Mexico: petrologic, geochemical and microthermometric constraints. Revista Mexicana de Ciencias Geológicas 24, 1–19.

Handin, J., Hager Jr., R.V., Friedman, M., Feather, J.N., 1963. Experimental deformation of sedimentary rocks under confining pressure; pore pressure tests. Bulletin of the American Association of Petroleum Geologists 47, 717–755.

Hennings, P. (Ed.), 2009. AAPG-SPE-Hedberg Research Conference on the geologic occurrence and hydraulic significance of fractures in reservoirs. Theme issue. AAPG Bulletin, 93, pp. 1407–1412.

Huang, Q., Angelier, J., 1989. Fracture spacing and its relation to bed thickness. Geological Magazine 126, 355–362.

Jensen, J.L., Lake, L.W., Corbett, P.W.M., Goggin, D.J., 1997. Statistics for Petroleum Engineers and Geoscientists. Prentice Hall Petroleum Engineering Series, New Jersey, 390 p.

Ji, S., Saruwatari, K., 1998. A revised model for the relationship between joint spacing and layer thickness. Journal of Structural Geology 20, 1495–1508.

Kleist, R., Hall, S.A., Evans, I., 1984. A paleomagnetic study of the Lower Cretaceous Cupido Limestone, northeast Mexico: evidence for local rotation within the Sierra Madre Oriental. Geological Society of America Bulletin 95, 55–60.

Ladeira, F.L., Price, N.J., 1981. Relationship between fracture spacing and bed thickness. Journal of Structural Geology 3, 179–183.

Laubach, S.E., 2003. Practical approaches to identifying sealed and open fractures. AAPG Bulletin 87, 561–579.

Laubach, S.E., Olson, J.E., Gross, M.R., 2009. Mechanical and fracture stratigraphy. AAPG Bulletin 93, 1413–1426.

Lehmann, C., Osleger, D.A., Montañez, I.P., 1998. Controls on cyclostratigraphy of Lower Cretaceous carbonates and evaporites, Cupido and Coahuila platforms,

northeastern Mexico. Journal of Sedimentary Research, Section B: Stratigraphy and Global Studies 68, 1109–1130.
Mandal, N., Deb, S.K., Khan, D., 1994. Evidence for a non-linear relationship between fracture spacing and layer thickness. Journal of Structural Geology 16, 1275–1281.
Marrett, R., 1996. Aggregate properties of fracture populations. Journal of Structural Geology 18, 169–631. 178.
Marrett, R., Aranda-García, M., 1999. Structure and kinematic development of the Sierra Madre Oriental fold-thrust belt, Mexico. In: Stratigraphy and Structure of the Jurassic and Cretaceous Platform and Basin Systems of the Sierra Madre Oriental, Monterrey and Saltillo Areas, Northeastern Mexico, a Field Book and Related Papers. South Texas Geological Society. . Special Publication for the Annual Meeting of the American Association of Petroleum Geologists and the SEPM. Society for Sedimentary Geology, San Antonio, p. 69-98.
Marrett, R., Laubach, S.E., 2001. Fracturing during diagenesis. In: Marrett, R. (Ed.), Monterrey Salient Genesis and Controls of Reservoir-Scale Carbonate Deformation. The University of Texas at Austin, Mexico, pp. 109–123. Bureau of Economic Geology, Field Trip Guidebook 28.
Monroy-Santiago, F., Laubach, S.E., Marrett, R., 2001. Preliminary diagenetic and stable isotope analyses of fractures in the Cupido Formation, Sierra Madre Oriental. In: Marrett, R. (Ed.), Genesis and Controls of Reservoir-Scale Carbonate Deformation, Monterrey Salient. The University of Texas at Austin, Mexico, pp. 83–107. Bureau of Economic Geology, Field Trip Guidebook 28.
Moros, J.G., 1999. Relationship Between Fracture Aperture and Length in Sedimentary Rocks. The University of Texas at Austin, Master's thesis, 120 p.
Morrow, D.W., 1982. Diagenesis 2. Dolomite, part 2: dolomitization models and ancient dolostones. Geoscience Canada 9, 95–107.
Mueller, M.C., 1991. Prediction of lateral variability in fracture intensity using multicomponent shear-wave surface seismic as a precursor to horizontal drilling in the Austin Chalk. Geophysical Journal International 107, 409–415.
Narr, W., 1991. Fracture density in the deep subsurface; techniques with application to Point Arguello Oil Field. AAPG Bulletin 75, 1300–1323.
Narr, W., 1996. Estimating average fracture spacing in subsurface rock. AAPG Bulletin 80, 1565–1586.
Narr, W., Suppe, J., 1991. Joint spacing in sedimentary rocks. Journal of Structural Geology 13, 1037–1048.
Nelson, R.A., 2001. Geologic Analysis of Naturally Fractured Reservoirs, second ed. Gulf Publishing, Houston, 320 p.
Nelson, R.A., Serra, S., 1995. Vertical and lateral variations in fracture spacing in folded carbonate sections and its relation to locating horizontal wells. The Journal of Canadian Petroleum Technology 34, 51–56.
Olson, J.E., Laubach, S.E., Lander, R.H., 2009. Natural fracture characterization in tight gas sandstones: integrating mechanics and diagenesis. AAPG Bulletin 93, 1535–1549.
Ortega, O.J., 2002. Fracture-Size Scaling and Stratigraphic Controls on Fracture Intensity. The University of Texas at Austin, PhD dissertation, 426 p.
Ortega, O.J., Marrett, R., Laubach, S.E., 2006. A scale-independent approach to fracture intensity and average fracture spacing. AAPG Bulletin 90, 193–208.
Philip, Z.G., Jennings Jr., J.W., Olson, J.E., Laubach, S.E., Holder, J., 2005. Modeling coupled fracture-matrix fluid flow in geomechanically simulated fracture networks. SPE Reservoir Evaluation and Engineering 8, 300–309.
Ramsay, J.G., 1980. The crack-seal mechanism of rock deformation. Nature 284, 135–139.
Rives, T., Razack, M., Petit, J.-P., Rawnsley, K.D., 1992. Joint spacing: analog and numerical simulations. Journal of Structural Geology 14, 925–937.
Sinclair, S.W., 1980. Analysis of Macroscopic Fractures on Teton Anticline, Northwestern Montana. Texas A&M University, Masters thesis, 102 p.
Swan, A.R.H., Sandilands, M., 1995. Introduction to Geological Data Analysis. Blackwell Science, Oxford, 446 p.
Wilson, J.L., Ward, W., Finneran, J., 1984. A Field Guide to Upper Jurassic and Lower Cretaceous Carbonate Platform and Basin Systems, Monterrey-Saltillo area, Northeast Mexico. Society of Economic Paleontologists and Mineralogists, GulfCoast Section, 76 p.
Wu, H., Pollard, D.D., 1995. An experimental study of the relationship between joint spacing and layer thickness. Journal of Structural Geology 17, 887–905.
Young, D.H., 1962. Statistical Treatment of Experimental Data. McGraw-Hill Book Company Inc., New York, 172 p.
Zahm, C.K., Zahm, L.C., Bellian, J.A., 2010. Integrated fracture prediction using sequence stratigraphy within a carbonate fault damage zone, Texas, USA. Journal of Structural Geology 32, 1363–1374.